EARTHQUAKE ENGINEERING AND STRUCTURAL DYNAMICS
Earthquake Engng. Struct. Dyn. **27**, 619–638 (1998)

A DISCRETE WAVENUMBER BOUNDARY ELEMENT METHOD FOR STUDY OF THE 3-D RESPONSE OF 2-D SCATTERERS

APOSTOLOS S. PAPAGEORGIOU* AND DUOLI PEI
Department of Civil Engineering, Rensselaer Polytechnic Institute, Troy, NY 12180-3590, U.S.A

SUMMARY

A mathematical formulation of the 2·5D elastodynamic scattering problem is presented and validated. The formulation is a straightforward extension of the Discrete Wave number Boundary Integral Equation Method (DWBIEM) originally proposed by Kawase[1] for 2D scattering problems and subsequently extended to the 3D problem by Kim and Papageorgiou.[2] It is demonstrated that the Green's function which is appropriate for a boundary formulation of the 2·5D elastodynamic scattering problem is the one corresponding to a unit force moving on a straight line with constant velocity. Such a Green's function is derived in the present study. The formulation may be used to study the wavefields in models of sedimentary deposits (e.g. valleys) or topography (e.g. canyons or ridges) with a 2D variation in structure but obliquely incident plane waves. The advantage of a 2·5D formulation is that it provides the means for calculations of 3D wavefields in scattering problems by requiring a storage comparable to that of the corresponding 2D calculations. © 1998 John Wiley & Sons, Ltd.

KEY WORDS: elastodynamic scattering; topography effects; sedimentary valley response; boundary element method; 2-5-D problem

1. INTRODUCTION

Various methods of elastodynamic calculations have been developed and applied in the study of site effects on earthquake ground motion. One possible classification of these computational methods is the following: (1) Discrete co-ordinate methods such as the Finite Difference Method,[3–6] the Finite Element Method,[7] the Boundary Integral Equation Method[8,9] and hybrids of the above methods;[10,11] and Dravinski, 1992; Regan and Harkrider, 1989; (2) Ray methods[12,13] Hong and (3) the Rayleigh Ansatz method (also referred to as the Aki-Larner method).[14,15] [For extensive lists of publications on the subject of numerical modelling of the elastodynamic response of geologic structures (such as basins, canyons and ridges) the reader is referred to the papers of Bouchon and Coutant[16] and Luco and de Barros.[17]

The models of the various geological structures that have been investigated range from simple local one-dimensional models[18] to complete regional three-dimensional models.[19,20]

However, full 3D calculations of general 3D geological formations are still very expensive to perform on a routine basis because of large memory requirements.

An economical approach, which does not require the same level of computational resources as the above 3D type of analyses, is to examine the 3D response of a model in which the structure of heterogeneity/scatterer is 2D. Such a model is referred to in the published literature as a 2·5*D model*. For example, mountain ranges and sedimentary valleys, by the very nature of their formation process, have a 2D structure.

* Correspondence to: Apostolos S. Papageorgiou, Department of Civil Engineering, Rensselaer Polytechnic Institute, Troy, NY 12180-3590, U.S.A. E-mail: papaga@socrates.eng.rpi.edu

Contract/grant sponsor: National Center for Earthquake Engineering Research; Contract/grant number: NCEER 93-2001, NCEER 94-2001, NCEER 95-2001
Contract/grant sponsor: NSF; Contract/grant number: ECE-86-07591

CCC 0098–8847/98/060619–20$17·50

Received 25 February 1997
Revised 12 August 1997

Several investigators have developed numerical methods to address such a 2·5D problem. Luco *et al.*[21] proposed a formulation for a 2·5D Indirect Boundary Integral Equation Method (IBIEM) based on the use of Green's functions corresponding to a moving point force in a layered viscoelastic half-space,[22,23] in order to obtain the 3D response of an infinitely long canyon, for plane elastic waves impinging at an arbitrary angle with respect to the axis of the canyon. We remind the reader that while the Direct Boundary Integral Equation Method (DBIEM) directly finds the unknown tractions and displacements at the boundary of the scatterer, the IBIEM searches a force distribution for which the radiated field satisfies the boundary conditions.[24] Luco *et al.*[21] use the IBIEM and locate sources off the surface of the canyon to displace singularities in the Green's functions from the surface. Boundary conditions are satisfied in a least-squares sense. The same numerical method was used by Luco and de Barros[25] to study the 3-D response of a class of cylindrical inclusions embedded in layered media and by Luco and de Barros[17] and de Barros and Luco[26] to study the response of sedimentary valleys to incident plane waves. They reported extensive and thoroughly checked numerical results, and they investigated the effects of horizontal and vertical angles of incidence, effects of layering, and dependence of the results on the frequency of the excitation.

In a parallel development, Pedersen *et al.*[27] extended an IBIEM, originally proposed by Sanchez-Sesma and Campillo[28] for the 2D problem, to the problem of the 3D response of 2D topographies. The above authors use a single-layer boundary integral representation of the diffracted elastic fields that is derived from Somigliana's identity. (Parenthetically, we mention that in connection with the above method, Yokoi and Takenaka[29] proposed a procedure to eliminate the non-physical waves which result from the fact that only a segment of *finite* length of the infinite free surface of the half-space, in which the scatterer is embedded, is discretized.) This approach is similar to the method proposed by Luco *et al.*[21] that was referenced above, except for the fact that the sources in this case are placed on the boundary, and the system of linear equations that arises from the discretization is solved directly. The method has been applied to (i) the study of amplification of seismic waves by ridges,[30] (ii) the problem of azimuth-dependent wave amplification in alluvial valleys[31] and (iii) the study of the 3D diffraction of long-period surface waves by 2D lithospheric structures.[32]

Considering the problem of the interaction of a 2D topography irregularity with the wavefield of a *point* source, Takenaka *et al.*[33] extended to the 2·5D case the IBIEM method introduced by Bouchon [34] and Gaffet and Bouchon[35] to study 2D topography problems. More recently, Takenaka and Kennett[36] proposed a 2·5D time-domain elastodynamic equation for seismic wavefields in models with a 2D variation in structure but obliquely incident plane waves. This approach was generalized by Takenaka and Kennett[37] for the case of non-planar waves (i.e. for the case when a source is present) and for general anisotropic media.

In a parallel effort, Furumura and Takenaka[38] developed an efficient 2·5D formulation for the pseudo-spectral method for point-source excitation and applied it successfully to modelling the waveforms recorded in a refraction survey.

Finally, other studies related to 2·5D elastodynamic scattering problems are those of Zhang and Chopra,[39,40] who used the DBIEM to determine the impedance matrix for a 3D foundation (such as that of an arch dam) supported on an infinitely long canyon of uniform cross-section cut in a homogeneous half-space. The DBIEM was used also by Khair *et al.*[41,42] and Liu[43] to study the response of cylindrical valleys to obliquely incident plane seismic waves.

In the present paper we present an alternative mathematical formulation of the 2·5D elastodynamic scattering problem based on the DBIEM. The formulation is a straightforward extension of the discrete wavenumber boundary integral equation method originally proposed by Kawase[1] for 2D scattering problems and subsequently extended to the 3D problem by Kim and Papageorgiou.[2] The mathematical formulation developed in the present paper has already been implemented by Pei and Papageorgiou,[44,45] Papageorgiou and Pei[46] and Zhang and Papageorgiou[47] in studies of the response of alluvial valleys, and Pei and Papageorgiou[48] in a study of topography effects. In the present study we *demonstrate* that the Green's function which is appropriate for a boundary formulation of the 2·5D elastodynamic scattering problem is the one corresponding to a point force moving on a straight line with constant velocity. (Incidentally, this type of Green's function has been used by Li *et al.*[49] in their study of reflection and transmission of obliquely incident plane surface waves by

an edge of a quarter-space using a boundary integral formulation.) We validate the formulation by comparing our results with those obtained by Luco *et al.*[21] Luco and de Barros,[17] and de Barros and Luco.[26] Finally, for purposes of demonstration, we present some simple examples of the time-domain response of scatterers (such as a canyon and a valley) to incident plane waves.

The method that is presented here is expected to be very accurate because no assumptions/approximations (other than the numerical evaluation of the integrals that appear in the formulation) are introduced. For instance, the IBIEMs that locate sources off the surface of the scatterer need to be calibrated for the optimum position of the sources. No such concern is necessary with the present method. Furthermore, the boundary conditions are satisfied exactly and not in a least-squares sense. Finally, because we use half-space Green's function, as opposed to full-space Green's functions, the zero-stress condition at the free surface of the half-space is automatically satisfied, avoiding thus the problem of artificial truncation of discretization of this surface. However, these advantages come at the expense of computational efficiency.

As pointed out in the text, several key results derived and used in the present formulation have been presented by other authors using different approaches to the problem. For instance, the expressions for the Green's functions corresponding to a moving point force [equations (32a)–(32c)] have been derived by Pedersen *et al.*,[27] using a different method than the one presented here. Similarly, the expression of the representation theorem, the one that is appropriate for the 2·5D problem [equation (12) below], was derived first by Zhang and Chopra.[39,40] However, the latter authors did not demonstrate (evidently because this was not necessary for their work) that the Green function that appeared in the expression was related to the response of a moving point source. Furthermore, formulations such as those presented by Pedersen et al.[27] [see equations (1), (2), (14) and (15) in their paper], and Luco *et al.*[21] [see equations (17) and (18) in their paper], state variant forms of the representation theorem (appropriate for an IBIEM), however without explaining how these expressions were derived and why the relevant Green functions that appear in the expressions should be those of a moving point force. (It should be stated, though, parenthetically, that Luco *et al.*[21] verbally point out the property of translational invariance of the wavefield along the axis of the scatterer, which is a key element in the mathematical derivation presented below.) Thus, in presenting our method of analysis we make it a point to present all these results in a unified way, demonstrating clearly all intermediate steps.

2. MATHEMATICAL FORMULATION OF THE PROBLEM

2.1. *Statement of the problem—elastodynamic integral formulation*

The model consists of an infinitely long viscoelastic inclusion/scatterer of arbitrary, but uniform cross-section embedded in a homogeneous (or horizontally layered) viscoelastic half-space. The geometry of the model used in the present study is shown in Figure 1 The excitation is represented by *plane* body waves impinging at an oblique angle with respect to the axis of the scatterer, or by *plane* surface waves incident from any azimuthal direction, as shown in Figure 1 Even though the model is two-dimensional, the response is three-dimensional and has the particular feature of repeating itself with a certain delay for different observers along the axis of the scatterer. Stating this differently, the response depends on the co-ordinate y along the axis of the scatterer and time t only through the combination $(y - Vt)$ where V is the apparent velocity of propagation of the excitation along the axis of the valley, i.e. the wavefield is *translationally invariant* with respect to y. By taking advantage of the translational invariance and by use of an appropriate Green's function, the three-dimensional physical problem may be reduced to a two-dimensional mathematical problem and thus lead to a considerably simpler solution.

The wave field in the absence of a scatterer is termed the *free-field solution* and is represented by $\mathbf{u}^{(o)}(\mathbf{x}, t)$ at a point defined by the position vector $\mathbf{x}$. The difference between the actual wave field $\mathbf{u}(\mathbf{x}, t)$ (i.e. the wave field in the presence of the scatterer) and the undisturbed wave $\mathbf{u}^{(o)}(\mathbf{x}, t)$, which would be present if the scatterer were not there, is termed the *scattered wave field* $\mathbf{u}^{(s)}(\mathbf{x}, t)$.[50] That is

$$\mathbf{u}(\mathbf{x}, t) = \mathbf{u}^{(o)}(\mathbf{x}, t) + \mathbf{u}^{(s)}(\mathbf{x}, t) \tag{1a}$$

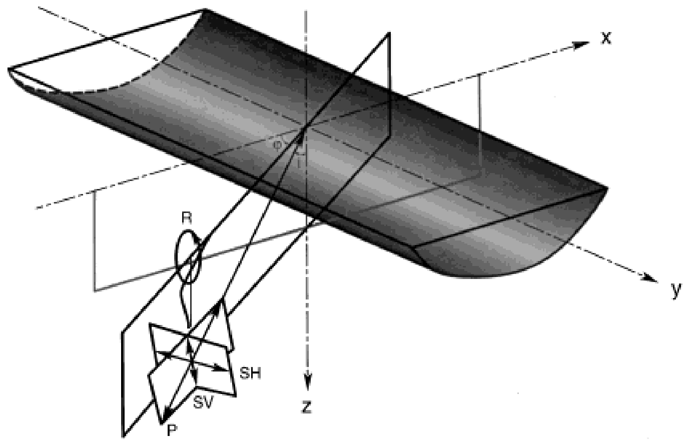

Figure 1. Scatterer with a 2D structure excited by obliquely incident plane body or surface waves. The angles φ and i are the azimuthal and incidence angles, respectively

or, for the case described above which satisfies the conditions of translational invariance of the wave field with respect to y,

$$\mathbf{u}(x, y - Vt, z) = \mathbf{u}^{(o)}(x, y - Vt, z) + \mathbf{u}^{(s)}(x, y - Vt, z) \tag{1b}$$

For the case of *harmonic* excitation of an incident wave, equations (1a) and (1b) may be written in terms of the amplitude of the *steady-state harmonic oscillations* as follows:

$$\mathbf{U}(\mathbf{x}, \omega) = \mathbf{U}^{(o)}(\mathbf{x}, \omega) + \mathbf{U}^{(s)}(\mathbf{x}, \omega) \tag{1c}$$

We begin by outlining the integral equation formulation of the boundary value problem at hand. In the initial steps of the presentation, our approach parallels that of Zhang and Chopra.[39,40] Our starting point is the reciprocal theorem (also referred to as the *dynamic Betti–Rayleigh theorem*[51]) for two reduced elastodynamic states in the absence of body forces.[52] Specifically, applying the reciprocal theorem over the region of the half-space, with one of the two elastodynamic states being the scattered wavefield $[\mathbf{U}^{(s)}(\mathbf{x}, \omega), \mathbf{T}^{(s)}_{(\mathbf{n})}(\mathbf{x}, \omega)]$ while the other one is the half-space Green's function $[\mathbf{G}^{H}(\mathbf{x}; \boldsymbol{\xi}, \omega), \mathbf{H}^{H}_{(\mathbf{n})}(\mathbf{x}; \boldsymbol{\xi}, \omega)]$ of the reduced field equation of elastodynamics for a stationary impulsive point force, we obtain

$$\int_{\Gamma}\int_{-\infty}^{+\infty} H^{H}_{(\mathbf{n})ji}(\mathbf{x}; \boldsymbol{\xi}_0, \omega)\, U^{(s)*}_{j}(\mathbf{x},\omega)\, \mathrm{d}y\, \mathrm{d}\Gamma = \int_{\Gamma}\int_{-\infty}^{+\infty} G^{H}_{ji}(\mathbf{x}; \boldsymbol{\xi}_0, \omega) T^{(s)*}_{(\mathbf{n})j}(\mathbf{x}, \omega)\, \mathrm{d}y\, \mathrm{d}\Gamma \tag{2}$$

where the star (*) represents a complex conjugate, $\mathbf{x}$ is the position vector of a point on the interface S of the scatterer with the half-space, $\boldsymbol{\xi}_0$ is the position vector of a point on curve Γ which is defined as the intersection of the xz-plane with the interface S appropriately indented to avoid singularity at $\boldsymbol{\xi}_0$, $U^{(s)}_{j}(\mathbf{x}, \omega)$ and $T^{(s)}_{(\mathbf{n})j}(\mathbf{x}, \omega)$ are the amplitudes of the jth component of the steady-state harmonic displacement and traction, respectively, of the scattered wavefield at point $\mathbf{x}$ of the half-space, $G^{H}_{ji}(\mathbf{x}; \boldsymbol{\xi}_0, \omega)$and $H^{H}_{(\mathbf{n})ji}(\mathbf{x}; \boldsymbol{\xi}_0, \omega)$ are the amplitudes of the jth component of the steady-state harmonic displacement and traction, respectively, at point $\mathbf{x}$ of the half-space Green's tensors (i.e. *Lamb's tensors*) due to a stationary point-force (i.e. a point-force the point of application of which does not change with time) applied in the ith direction at point $\boldsymbol{\xi}_0$, and $\mathbf{n}$ is an outward pointing unit normal vector of the interface boundary S. The scattered wavefield satisfies the *radiation conditions* and thus the integral over the surface which bounds the half-space at infinity is equal to zero.[52] (Parenthetically, we state at the outset that we use both indicial notation and unabridged notation

in terms of x, y, z, interchangeably, with the tacit understanding that the values of 1, 2, 3 of a subscript correspond to x, y, z, respectively.)

In view of the fact that the system geometry has a uniform cross-section along the y-axis, we express the field variables $U_j^{(s)}(\mathbf{x},\omega)$ and $T_{(\mathbf{n})j}^{(s)}(\mathbf{x},\omega)$ in terms of their Fourier integral representations. Thus, for displacements

$$\tilde{U}_j^{(s)}(x,k_y,z,\omega)=\int_{-\infty}^{+\infty} U_j^{(s)}(\mathbf{x},\omega)\,\mathrm{e}^{\mathrm{i}k_y y}\,\mathrm{d}y \tag{3a}$$

and

$$U_j^{(s)}(\mathbf{x},\omega)=\frac{1}{2\pi}\int_{-\infty}^{+\infty}\tilde{U}_j^{(s)}(x,k_y,z,\omega)\mathrm{e}^{-\mathrm{i}k_y y}\,\mathrm{d}k_y \tag{3b}$$

and the corresponding expressions are valid for the traction components $\tilde{T}_{(\mathbf{n})j}^{(s)}\left(x,k_y,z,\omega\right)$, as well as for the components of the Green's tensors $G_{ji}^{\mathrm{H}}(\mathbf{x};\boldsymbol{\xi}_0,\omega)$ and $H_{(\mathbf{n})ji}^{\mathrm{H}}(\mathbf{x};\boldsymbol{\xi}_0,\omega)$.

Substituting equation (3b) and the corresponding expression for traction $\tilde{T}_{(\mathbf{n})j}^{(s)}\left(x,k_y,z,\omega\right)$ in equation (2), interchanging the order of integration, and making use of the definitions of Fourier transforms of $G_{ji}^{\mathrm{H}}(\mathbf{x};\boldsymbol{\xi}_0,\omega)$ and $H_{(\mathbf{n})ji}^{\mathrm{H}}(\mathbf{x};\boldsymbol{\xi}_0,\omega)$, we obtain

$$\int_\Gamma\int_{-\infty}^{+\infty}\left[\tilde{H}_{(\mathbf{n})ji}^{\mathrm{H}}\left(x,k_y,z;\boldsymbol{\xi}_0,\omega\right)\tilde{U}_j^{(s)*}\left(x,k_y,z,\omega\right)-G_{ji}^{\mathrm{H}}\left(x,k_y,z;\boldsymbol{\xi}_0,\omega\right)\tilde{T}_j^{(s)*}\left(x,k_y,z,\omega\right)\right]\mathrm{d}k_y\,\mathrm{d}\Gamma=0 \tag{4}$$

At this point we exploit the *translational invariance* of the wavefield with respect to the y-axis that was discussed previously. Considering, for example, the displacement field $u_j^{(s)}(x,y-Vt,z)$, it may be easily demonstrated that

$$\tilde{U}_j^{(s)}\left(x,k_y,z,\omega\right)\equiv\int_{-\infty}^{+\infty}\int_{-\infty}^{+\infty}u_j^{(s)}(x,y-Vt,z)\,\mathrm{e}^{\mathrm{i}k_y y}\mathrm{e}^{-\mathrm{i}\omega t}\,\mathrm{d}y\,\mathrm{d}t=\tilde{u}_j^{(s)}\left(x,k_y,z\right)2\pi\delta\left(Vk_y-\omega\right) \tag{5}$$

$$\tilde{u}_j^{(s)}\left(x,k_y,z\right)=\int_{-\infty}^{+\infty}u_j^{(s)}\left(x,y',z\right)\mathrm{e}^{\mathrm{i}k_y y'}\,\mathrm{d}y' \tag{6}$$

where $\delta(\cdot)$ is the Dirac delta function.

Equation (6) in essence represents the spatial Fourier transform (i.e. with respect to the y-co-ordinate) of a snapshot of the wavefield at the time instant $t=0$.

From equation (3b) and (5) it follows that

$$U_j^{(s)}(\mathbf{x},\omega)=\frac{1}{V}\tilde{u}_j^{(s)}\left(x,\frac{\omega}{V},z\right)\mathrm{e}^{-\mathrm{i}(\omega/V)y} \tag{7}$$

Corresponding equations to equations (5)–(7) exist also for the components of traction $t_{(\mathbf{n})j}^{(s)}(x,y-Vt,z)$. Substituting equation (5) and the corresponding equation for traction in equation (4), we obtain

$$\int_\Gamma\int_{-\infty}^{+\infty}2\pi\delta\left(Vk_y-\omega\right)\left[\tilde{H}_{(\mathbf{n})ji}^{\mathrm{H}}\left(x,k_y,z;\boldsymbol{\xi}_0,\omega\right)\tilde{u}_j^{(s)*}\left(x,k_y,z\right)-\tilde{G}_{ji}^{\mathrm{H}}\left(x,k_y,z;\boldsymbol{\xi}_0,\omega\right)\tilde{t}_{(\mathbf{n})j}^{(s)*}\left(x,k_y,z\right)\right]\mathrm{d}\,k_y\,\mathrm{d}\Gamma=0 \tag{8}$$

As it will become evident below [see equations (30a)–(30d)], $\tilde{G}_{ji}^{\mathrm{H}}\left(x,k_y,z;\boldsymbol{\xi}_0,\omega\right)2\pi\delta\left(Vk_y-\omega\right)$ and $\tilde{H}_{(\mathbf{n})ji}^{\mathrm{H}}\left(x,k_y,z;\boldsymbol{\xi}_0,\omega\right)2\pi\delta\left(Vk_y-\omega\right)$ represent in the (ω,k_y) domain the displacement and traction half-space Green's tensors, respectively, for a point force moving parallel to the y-axis with a constant velocity V. The presence

of the Dirac delta function in the integrand of equation (8), permits the analytical evaluation of the integral over k_y. Thus, from equation (8) we obtain

$$\int_{\Gamma}\left[H^{\mathrm{H}'}_{(\mathbf{n})ji}(\mathbf{x}_0;\boldsymbol{\xi}_0,\omega)\cdot\frac{1}{V}\tilde{u}^{(\mathrm{s})^*}_j\left(x,\frac{\omega}{V},z\right)-G^{\mathrm{H}'}_{ji}(\mathbf{x}_0;\boldsymbol{\xi}_0,\omega)\cdot\frac{1}{V}\tilde{t}^{(\mathrm{s})^*}_{(\mathbf{n})j}\left(x,\frac{\omega}{V},z\right)\right]\mathrm{d}\Gamma=0 \tag{9}$$

where $G^{\mathrm{H}'}_{ji}(\mathbf{x};\boldsymbol{\xi}_0,\omega)=\tilde{G}^{\mathrm{H}}_{ji}(\mathbf{x},\omega/V,z;\boldsymbol{\xi}_0\omega)\,\mathrm{e}^{-\mathrm{i}(\omega/V)y}$ and $H^{\mathrm{H}'}_{(\mathbf{n})ji}(\mathbf{x};\boldsymbol{\xi}_0,\omega)=\tilde{H}^{\mathrm{H}}_{(\mathbf{n})ji}(x,\omega/V,z;\boldsymbol{\xi}_0,\omega)\,\mathrm{e}^{-\mathrm{i}(\omega/V)y}$ are the amplitudes of the steady-state harmonic displacement and traction Green tensors, respectively, corresponding to a point force moving parallel to the y-axis with a constant velocity V, and $\mathbf{x}_0=(\mathbf{x},0,z)$ (i.e. a point on curve Γ on the xz-plane).

Evaluating equation (7) at a point $\mathbf{x}=\mathbf{x}_0=(x,0,z)$ and combining it with equation (9) we obtain

$$\int_{\Gamma}\left[H^{\mathrm{H}'}_{(\mathbf{n})ji}(\mathbf{x}_0;\boldsymbol{\xi}_0,\omega)\cdot U^{(\mathrm{s})*}_j(\mathbf{x}_0,\omega)-G^{\mathrm{H}'}_{ji}(\mathbf{x}_0;\boldsymbol{\xi}_0,\omega)\cdot T^{(\mathrm{s})*}_j(\mathbf{x}_0,\omega)\right]\mathrm{d}\Gamma=0 \tag{10}$$

At this point we remind the reader that the curve Γ is indented so as to avoid the singularity at point $\boldsymbol{\xi}_0$. The indentation is represented by a circular arc Γ_ρ of radius ρ . Now, noticing that $\lim_{\rho\to 0}\int_{\Gamma_\rho}H^{\mathrm{H}'}_{(\mathbf{n})ji}(\mathbf{x}_0;\boldsymbol{\xi}_0,\omega)\,\mathrm{d}\Gamma=C_{ij}/V$, equation (10) reduces to

$$C_{ij}\frac{1}{V}U^{(\mathrm{s})*}_j(\boldsymbol{\xi}_0,\omega)=\int_{\Gamma}G^{\mathrm{H}'}_{ji}(\mathbf{x}_0;\boldsymbol{\xi}_0,\omega)\,T^{(\mathrm{s})*}_j(\mathbf{x}_0,\omega)\,\mathrm{d}\Gamma-P\int_{\Gamma}H^{\mathrm{H}'}_{(\mathbf{n})ji}(\mathbf{x}_0;\boldsymbol{\xi}_0,\omega)U^{(\mathrm{s})*}_j(\mathbf{x}_0,\omega)\,\mathrm{d}\Gamma \tag{11}$$

where $P\int_{\Gamma}$ denotes that the line integral is defined in the sense of the Cauchy principle value (CPV), and the coefficient tensor C_{ij} of the free term is determined by the boundary shape around $\boldsymbol{\xi}_0$ and is equal to $(1/2)\,\delta_{ij}$ (where δ_{ij} is the Kronecker symbol) in case of a smooth boundary.[53–55]

Combining equations (1c) and (11) we obtain the following boundary integral equation for incident wave analyses (for a detailed derivation of this equation see, for example, References 1 and 56–58),

$$\begin{aligned}C_{ij}U^*_j(\boldsymbol{\xi}_0,\omega)=&\int_{\Gamma}G^{\mathrm{H}'}_{ji}(\mathbf{x}_0;\boldsymbol{\xi}_0,\omega)\,VT^*_j(\mathbf{x}_0,\omega)\,\mathrm{d}\Gamma\\&-P\int_{\Gamma}H^{\mathrm{H}'}_{(\mathbf{n})ji}(\mathbf{x}_0;\boldsymbol{\xi}_0,\omega)\,VU^*_j(\mathbf{x}_0,\omega)\,\mathrm{d}\Gamma+U^{(0)*}_i(\boldsymbol{\xi}_0,\omega)\end{aligned} \tag{12}$$

Equation (12)—referred to as *Somigliana identity*[56,54]—is the mathematical statement of *Huygen's principle* for steady-state elastic waves.[56,59–61] [An identical expression to equation (12) is valid but without the stars ($*$) (i.e. without taking the complex conjugates of the respective variables) (see Reference 52, pp. 432–433)]. To solve this equation for arbitrary boundary shape and conditions, the discretization of both boundary shape and values $U^*_j(\boldsymbol{\xi}_0,\omega)$ and $T^*_j(\boldsymbol{\xi}_0,\omega)$ should be introduced in the same manner as in the finite-element method.[62,63] The simplest boundary element is a constant-value line element (a constant-value line element is an element that is a straight-line segment and the field variables U_j and T_j are assumed to be constant over its length), which allows expression of the integral equation by means of

$$C_{ij}U^*_j[n,\omega]=\sum_{m=1}^{M}\tilde{G}_{ji}[m;n]\,T^*_j[m]-\sum_{m=1}^{M}\tilde{H}_{ji}[m;n]\,U^*_j[m]+U^{(0)*}_i[n] \tag{13}$$

In this equation, M is the total number of elements, n represents the element that is intercepted at its node by the axis on which the moving point force is acting, $U^{(0)*}_i[n]$ represents the value of the ith component of the free-field displacement evaluated at the node (i.e. centroid) of the nth element, and $\tilde{G}_{ji}[m;n]$ and $\tilde{H}_{ji}[m;n]$

represent the element integrations—over the length L_m of the mth element—expressed by

$$\tilde{G}_{ji}[m;n] = \int_{L_m} V \cdot G_{ji}^{\mathrm{H}'}(\mathbf{x}_{0m};\xi_{0n},\omega)\,\mathrm{d}L(\mathbf{x}_{0m}) \tag{14}$$

and the corresponding expression for the traction tensor.

By combining equations for different n, we obtain the final simultaneous linear equations to be solved for the unknown boundary values over the boundary Γ of the irregularity/scatterer.

2.2. '2·5D' Green functions

In the following, we present a derivation of the Green tensors of displacement and traction for a point force *moving* with constant velocity along a straight line in an isotropic, homogeneous elastic space. The derivation parallels the one originally proposed by Lamb[64] and subsequently developed by Bouchon[65] for a *stationary* point force.

Let us define a Cartesian co-ordinate system (x,y,z) in an isotropic, homogeneous elastic space and let us consider a point force of unit strength, acting in the direction of the m-axis ($m = x,y,z$) and moving on the y-axis with constant velocity V. Such a source of excitation is expressed mathematically as

$$f_i(\mathbf{x},t) = \delta_{im}\delta(x)\,\delta(y - Vt)\,\delta(z) \tag{15}$$

where $f_i(\mathbf{x},t)$ are the components of the point force acting at a point defined by the position vector $\mathbf{x}$ at time t, δ_{im} is the Kronecker symbol and $\delta(\cdot)$ is the Dirac delta function.

Following Lamb[64] and Bouchon,[65] we simulate the body force as a field discontinuity, and in particular, as a discontinuity in an appropriately selected component of traction. The elastodynamic equivalence of a body force and a traction discontinuity was formally demonstrated by Burridge and Knopoff[66] (see also Reference 67) and is expressed by the following equation:

$$\mathbf{f}^{[\mathbf{t}]}(\boldsymbol{\eta},t) = -\int\int_{\Sigma}[\mathbf{t}(\mathbf{u}(\xi,t),\mathbf{n})]\,\delta(\boldsymbol{\eta}-\boldsymbol{\xi})\,\mathrm{d}\Sigma(\boldsymbol{\xi}) \tag{16}$$

where $[\mathbf{t}] \equiv \mathbf{t}(\boldsymbol{\xi},t)|_{\Sigma^+} - \mathbf{t}(\boldsymbol{\xi},t)|_{\Sigma^-}$ represents the traction discontinuity at time t at a point defined by the position vector $\boldsymbol{\xi}$ on a plane Σ defined by the unit normal vector $\mathbf{n}$.

Thus, for instance, a point force of strength F acting along the direction of the positive z-axis and moving on the y-axis with constant velocity V, may be simulated by a traction discontinuity

$$[\mathbf{t}] = -(0,0,F)\,\delta(x)\,\delta(y - Vt) \tag{17}$$

i.e. the stress components τ_{zx},τ_{zy} are continuous and this is a jump discontinuity in τ_{zz}, i.e.

$$[\tau_{zz}] = -F\delta(x)\,\delta(y - Vt) \tag{18}$$

Let $\left[\tilde{\tilde{\tau}}_{zz}\right]$ be the space–time Fourier transform of $[\tau_{zz}]$. Then, from equation (18), we obtain

$$\left[\tilde{\tilde{\tau}}_{zz}\right] = \int\int_{-\infty}^{+\infty}\int [\tau_{zz}]\,\mathrm{e}^{\mathrm{i}(k_x x + k_y y - \omega t)}\,\mathrm{d}x\,\mathrm{d}y\,\mathrm{d}t = -2\pi F\delta\left(Vk_y - \omega\right) \tag{19}$$

Applying the inverse space–time Fourier transform, $[\tau_{zz}]$ may be expressed as

$$[\tau_{zz}] = \frac{1}{(2\pi)^3}\int\int_{-\infty}^{+\infty}\int -2\pi F\delta\left(Vk_y - \omega\right)\mathrm{e}^{\mathrm{i}(\omega t - k_x x - k_y y)}\,\mathrm{d}k_x\,\mathrm{d}k_y\,\mathrm{d}\omega \tag{20}$$

Our analysis up to this point suggests that our original problem of finding the displacement and stress field due to a point force acting along the z-axis and moving on the y-axis with constant velocity V may be solved by obtaining the solution to the following boundary value problem:

$$\tau_{zz}(z=+0)-\tau_{zz}(z=-0)=-2\pi F\delta\left(Vk_y-\omega\right)\mathrm{e}^{\mathrm{i}(\omega t-k_x x-k_y y)} \tag{21a}$$

$$\tau_{zx}(z=+0)=\tau_{zx}(z=-0) \tag{21b}$$

$$\tau_{zy}(z=+0)=\tau_{zy}(z=-0) \tag{21c}$$

$$\mathbf{u}(z=+0)=\mathbf{u}(z=-0) \tag{22}$$

and by superposing such solutions in the form expressed by equation (20).

To solve the boundary value problem stated by equations (21a)–(21c) and (22), we express the displacement field using the *Stokes–Helmholtz* resolution as

$$\mathbf{u}=\nabla\varphi+\nabla\times\boldsymbol{\psi} \tag{23}$$

where $\varphi\,(\mathbf{x},t)$ and $\boldsymbol{\psi}\,(\mathbf{x},t)$ are, respectively, scalar- and vector-value functions defined as

$$\varphi(\mathbf{x},t)=\Phi(\mathbf{x},\omega)\,\mathrm{e}^{\mathrm{i}\omega t},\qquad \boldsymbol{\psi}(\mathbf{x},t)=\boldsymbol{\Psi}(\mathbf{x},\omega)\,\mathrm{e}^{\mathrm{i}\omega t} \tag{24a,b}$$

and referred to as *Lamé potentials*.[52,67] The amplitudes $\Phi(mathbf fx,\omega)$ and $\boldsymbol{\Psi}(\mathbf{x},\omega)$ of the steady-state oscillations expressed by equation (24) satisfy the *reduced wave equations*

$$\left(\nabla^2+k_\alpha^2\right)\Phi=0;\qquad \left(\nabla^2+k_\beta^2\right)\boldsymbol{\Psi}=\mathbf{0} \tag{25a,b}$$

where $k_\alpha=(\omega/\alpha)$ and $k_\beta=(\omega/\beta)$, and $\boldsymbol{\Psi}(\mathbf{x},\omega)$ obeys the additional condition (*gauge condition*),

$$\nabla\cdot\boldsymbol{\Psi}=\mathbf{0} \tag{26}$$

Notice that equations (26a) and (26b) are homogeneous wave equations because the reformulated problem that we want to solve, as expressed by equations (21a)–(21c) and (22), does not involve explicitly any body forces.

Solving the boundary value problem posed by equations (21)–(26), and superposing the solution, in the fashion expressed by equation (20), we obtain the Lamé potentials of the displacement field radiated from a point force of strength $F=1$, that is acting along the positive z-axis and moving on the y-axis with constant velocity V. The components of the potentials are given by the following expressions:

$$\Phi^z=\frac{\operatorname{sgn}(z)}{8\pi^2k_\beta^2\mu}\int_{-\infty}^{+\infty}\int_{-\infty}^{+\infty}2\pi\delta\left(Vk_y-\omega\right)\exp\left(-\mathrm{i}k_x x-\mathrm{i}k_y y-\mathrm{i}\nu\,|z|\right)\mathrm{d}k_x\,\mathrm{d}k_y \tag{27a}$$

$$\Psi_1^z=\frac{1}{8\pi^2k_\beta^2\mu}\int_{-\infty}^{+\infty}\int_{-\infty}^{+\infty}2\pi\delta\left(Vk_y-\omega\right)\frac{k_y}{\gamma}\exp\left(-\mathrm{i}k_x x-\mathrm{i}k_y y-\mathrm{i}\gamma\,|z|\right)\mathrm{d}k_x\,\mathrm{d}k_y \tag{27b}$$

$$\Psi_2^z=\frac{1}{8\pi^2k_\beta^2\mu}\int_{-\infty}^{+\infty}\int_{-\infty}^{+\infty}2\pi\delta\left(Vk_y-\omega\right)\frac{k_x}{\gamma}\exp\left(-\mathrm{i}k_x x-\mathrm{i}k_y y-\mathrm{i}\gamma\,|z|\right)\mathrm{d}k_x\,\mathrm{d}k_y \tag{27c}$$

$$\Psi_3^z=0 \tag{27d}$$

where the superscript z of the potentials indicates the direction of action of the moving point force, and $\nu=\left(k_\alpha^2-k_x^2-k_y^2\right)^{1/2}$, $\operatorname{Im}\nu\leqslant 0$; $\gamma=\left(k_\beta^2-k_x^2-k_y^2\right)^{1/2}$, $\operatorname{Im}\gamma\leqslant 0$.

It should be pointed out that the above expressions are identical to the expressions obtained by Bouchon[65] [equation (13) of his paper] except for the factor $2\pi\delta\left(Vk_y-\omega\right)$, which appears in all the integrands and

allows for the analytical evaluation of the integral over k_y using the properties of the Dirac delta function. [This justifies our statement made previously in going from equation (8) to equation (9).]

Thus, integrating first with respect to k_y and then making use of the following formula:[68]

$$H_0^{(2)}\left(a\left(z^2+b^2\right)^{1/2}\right) = -\left(\frac{1}{\pi \mathrm{i}}\right)\int_{-\infty}^{+\infty} \mathrm{e}^{\pm \mathrm{i}bu - z\left(u^2-a^2\right)^{1/2}} \frac{\mathrm{d}u}{\left(u^2-a^2\right)^{1/2}} \tag{28}$$

we obtain

$$\Phi^z = \frac{k_1 z}{4\mathrm{i}k_\beta^2\mu}\frac{1}{r}H_1^{(2)}(k_1 r)\frac{\mathrm{e}^{-\mathrm{i}(\omega/V)y}}{V} \tag{29a}$$

$$\Psi_1^z = -\frac{(\omega/V)}{4k_\beta^2\mu}H_0^{(2)}(k_2 r)\frac{\mathrm{e}^{-\mathrm{i}(\omega/V)y}}{V} \tag{29b}$$

$$\Psi_2^z = \frac{k_2 x}{4\mathrm{i}k_\beta^2\mu}\frac{1}{r}H_1^{(2)}(k_2 r)\frac{\mathrm{e}^{-\mathrm{i}(\omega/V)y}}{V} \tag{29c}$$

$$\Psi_3^z = 0 \tag{29d}$$

where $r = \left(x^2+z^2\right)^{1/2}$, $k_1 = \left[k_\alpha^2 - (\omega/V)^2\right]^{1/2}$, and $k_2 = \left[k_\beta^2 - (\omega/V)^2\right]^{1/2}$, with $\operatorname{Im} k_1 \leqslant 0$ and $\operatorname{Im} k_2 \leqslant 0$.

A similar development may be followed for a force acting along the x-axis or along the y-axis, and moving with constant velocity V on the y-axis.

Specifically, a force acting in the direction of the x-axis may be simulated by a traction discontinuity of the form $[\tau_{zx}] = -\delta(x)\,\delta(y-Vt)$ and the corresponding expressions of the Lamé potentials for displacement are the following:

$$\Phi^x = \frac{k_1 x}{4\mathrm{i}k_\beta^2\mu}\frac{1}{r}H_1^{(2)}(k_1 r)\frac{\mathrm{e}^{-\mathrm{i}(\omega/V)y}}{V} \tag{30a}$$

$$\Psi_1^x = 0 \tag{30b}$$

$$\Psi_2^x = -\frac{k_2 x}{4\mathrm{i}k_\beta^2\mu}\frac{1}{r}H_1^{(2)}(k_2 r)\frac{\mathrm{e}^{-\mathrm{i}(\omega/V)y}}{V} \tag{30c}$$

$$\Psi_3^x = -\frac{(\omega/V)}{4k_\beta^2\mu}H_0^{(2)}(k_2 r)\frac{\mathrm{e}^{-\mathrm{i}(\omega/V)y}}{V} \tag{30d}$$

while a force acting in the direction of the y-axis may be simulated by a traction discontinuity of the form $\left[\tau_{zy}\right] = -\delta(x)\,\delta(y-Vt)$ and the corresponding expressions of the Lamé potentials for displacement are the following:

$$\Phi^y = \frac{(\omega/V)}{4k_\beta^2\mu}H_0^{(2)}(k_1 r)\frac{\mathrm{e}^{-\mathrm{i}(\omega/V)y}}{V} \tag{31a}$$

$$\Psi_1^y = \frac{k_2 z}{4\mathrm{i}k_\beta^2\mu}\frac{1}{r}H_1^{(2)}(k_2 r)\frac{\mathrm{e}^{-\mathrm{i}(\omega/V)y}}{V} \tag{31b}$$

$$\Psi_2^y = 0 \tag{31c}$$

$$\Psi_3^y = -\frac{k_2 x}{4\mathrm{i}k_\beta^2\mu}\frac{1}{r}H_1^{(2)}(k_2 r)\frac{\mathrm{e}^{-\mathrm{i}(\omega/V)y}}{V} \tag{31d}$$

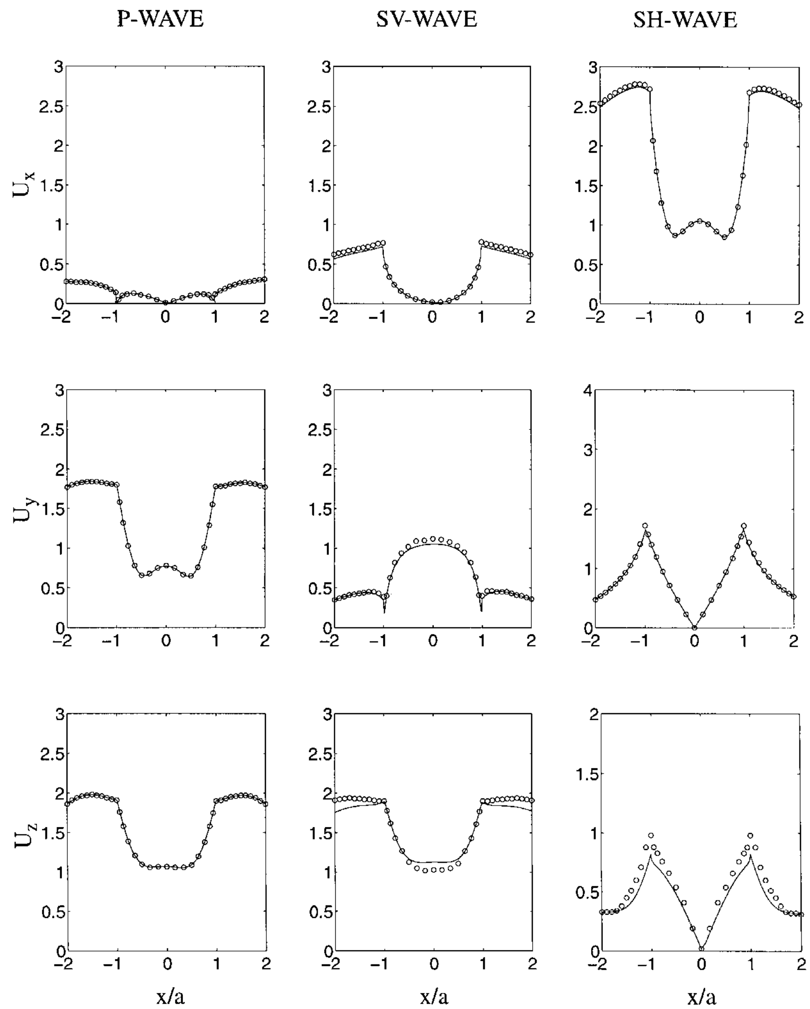

Figure 2. Scattering of body waves by a semi-circular canyon of radius *a*. Comparison of the results obtained by the present method (lines) with the results of Luco *et al.*[21] (represented by circles) for P-, SV- and SH-waves: $\varphi = 89°$, $i = 45°$, $\eta = 0{\cdot}5$

From equations (23), (24a), (24b), (29a)–(29d), (30a)–(30d) and (31a)–(31d) we obtain the displacement field (the time dependence expressed by $e^{i\omega t}$ is implied)

$$G_{ij}^{F'} = \frac{1}{8i\rho}\left[\delta_{ij}A - \left(2\gamma_i\gamma_j - \delta_{ij}\right)B\right]\frac{e^{-i(\omega/V)y}}{V} \quad (i, j = 1, 3) \tag{32a}$$

$$G_{2j}^{F'} = G_{j2}^{F'} = \frac{1}{4\rho V}\gamma_j C \frac{e^{-i(\omega/V)y}}{V} \quad (j = 1, 3) \tag{32b}$$

$$G_{22}^{F'} = \frac{1}{4i\rho}\left[\left(\frac{1}{\beta^2} - \frac{1}{V^2}\right)H_0^{(2)}(k_2 r) + \frac{1}{V^2}H_0^{(2)}(k_1 r)\right]\frac{e^{-i(\omega/V)y}}{V} \tag{32c}$$

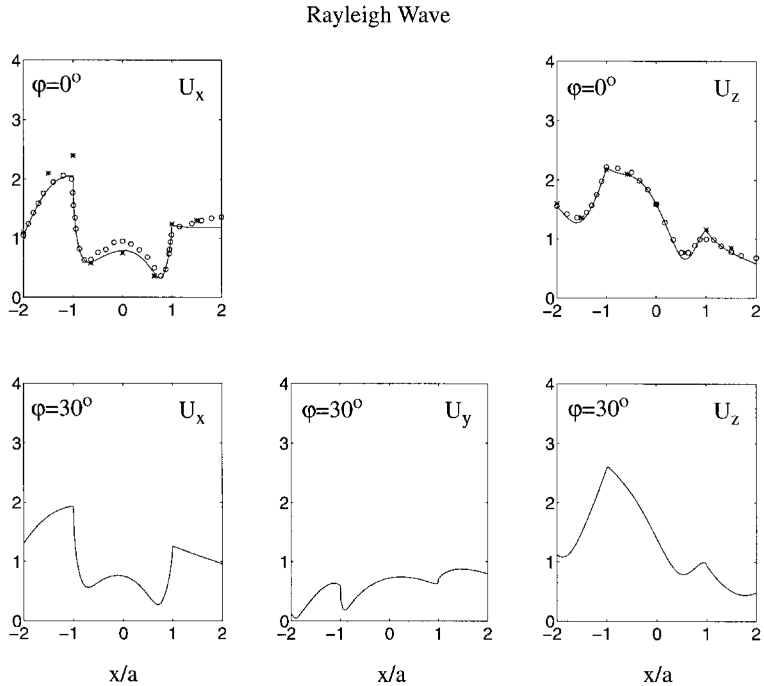

Figure 3. Scattering of a Rayleigh wave by a semi-circular canyon of radius a for two different values of the azimuthal angle φ: 0 and 30°. For the case $\varphi = 0$, the results obtained by the present method (lines) are compared with those obtained by Sanchez-Sesma *et al.* (circles) and Wong (asterisks). Non-dimensional parameter $\eta = 0{\cdot}5$

where $\gamma_i = x_i/r$ are the direction cosines, and

$$A = \left(\frac{1}{\alpha^2} - \frac{1}{V^2}\right) H_0^{(2)}(k_1 r) + \left(\frac{1}{\beta^2} + \frac{1}{V^2}\right) H_0^{(2)}(k_2 r) \tag{33a}$$

$$B = \left(\frac{1}{\alpha^2} - \frac{1}{V^2}\right) H_2^{(2)}(k_1 r) - \left(\frac{1}{\beta^2} - \frac{1}{V^2}\right) H_2^{(2)}(k_2 r) \tag{33b}$$

$$C = \left(\frac{1}{\beta^2} - \frac{1}{V^2}\right)^{1/2} H_1^{(2)}(k_2 r) - \left(\frac{1}{\alpha^2} - \frac{1}{V^2}\right)^{1/2} H_1^{(2)}(k_1 r) \tag{33c}$$

The corresponding components of the Green's traction tensor $H_{ij}^{F'}$ are obtained in a straightforward way by applying Hooke's law and may be found in Pei.[69]

Notice that the expressions (32a)–(32c) of the displacement Green tensor have a common factor $\exp[-\mathrm{i}(\omega/V)\,y]/V$. When these expressions are evaluated for $y = 0$ and combined with equation (12), then the complex exponential term becomes equal to 1 and the $(1/V)$ term cancels the V term that appears in the integrands of equation (12). For the 2D case (i.e. when the azimuthal angle φ of the incident plane wave excitation is equal to zero; Figure 1), the apparent velocity V becomes infinite and thus $VG_{2j}^{F'} = 0$ $(j = 1, 3)$ (i.e. the in-plane and out-of-plane responses are decoupled) and the expressions of $VG_{2j}^{F'}$ $(i, j = 1, 3)$ and $VG_{22}^{F'}$ tend to the displacement Green tensors appropriate for the 2D problem. The expressions given by equations (32a)–(32c) and (33a)–(33c) are identical to those derived by Pedersen *et al.*[27,30] except for the $(1/V)$ factor that appears in our expressions, i.e. the components of the displacement Green tensor for a point moving

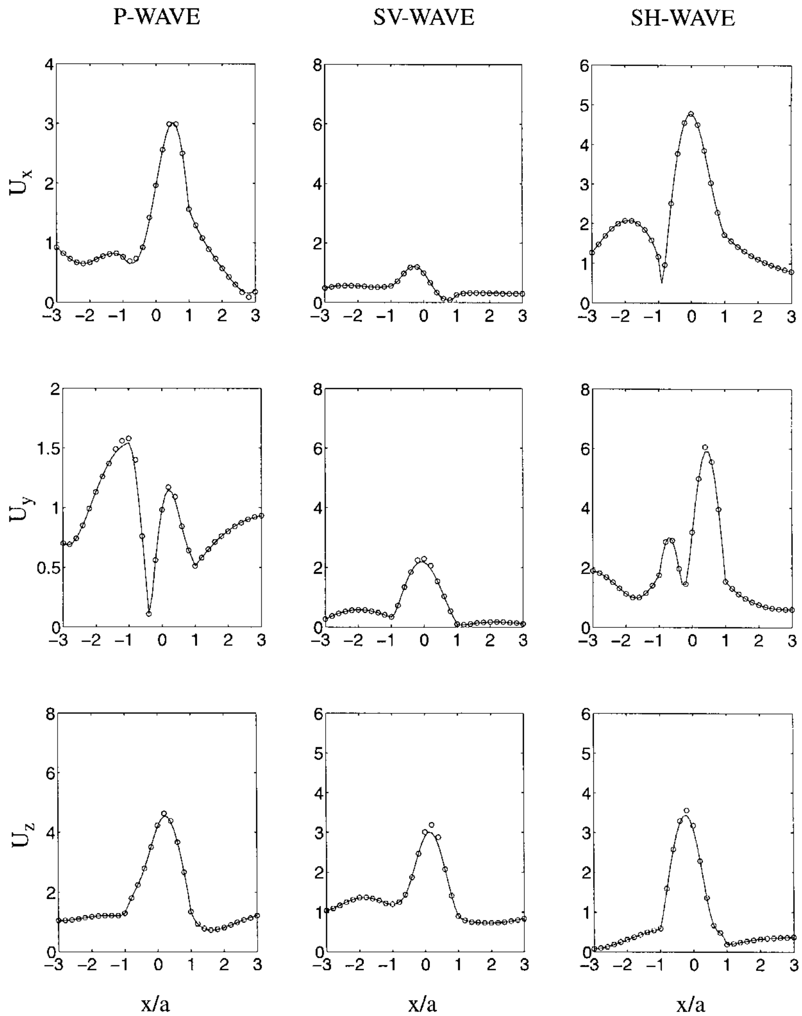

Figure 4. Scattering of body waves by a semi-circular valley of radius a. Comparison of surface displacement amplitudes using the present approach (lines) with those obtained by de Barros and Luco (1995) (circles). $\varphi = 45°$, $i = 60°$, $\eta = 0{\cdot}5$

force that Pedersen *et al.*[27,30] derived are really $VG_{ij}^{F'}$. Similar comments to those made above apply also for the traction tensor.

So far we have considered a point force, the point of application of which was assumed to move on the y-axis. Now, if we consider a point force moving on a line parallel to the y-axis that intercepts the xz-plane at point $(\xi_1, 0, \xi_3)$, then the expressions of the Green tensors that we derived (i.e. equations (32a)–(32c) are still valid, with the variable r defined as $r = [(x - \xi_1)^2 + (z - \xi_3)^2]^{1/2}$. The half-space Green tensors may be derived following a procedure proposed by Kawase[57] (see also Reference 70), and briefly outlined by Kim and Papageorgiou.[2] The expressions for the traction Green tensor $\mathrm{H}^{\mathrm{H}'}_{(\mathbf{n})ij}(\mathbf{x}; \boldsymbol{\xi}_0, \omega)$ may easily be derived, given the displacement Green tensor, from Hooke's law. Element integrations can be performed exactly as in the 2D case.[1,69]

Finally, the *apparent velocity of propagation of the excitation V* along the y-axis, takes the following values, depending on the type of incident plant wave: (i) for P-waves, $V = \alpha/(\sin i \sin \varphi)$; (ii) for SH- and

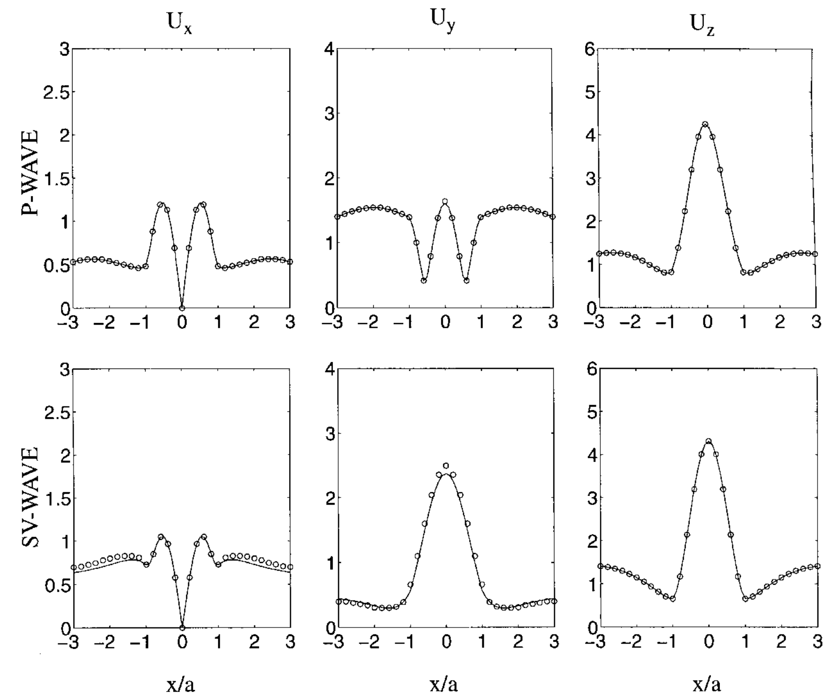

Figure 5. Same as Figure 4, but for $\varphi = 90°$, $i = 60°$, $\eta = 0{\cdot}5$

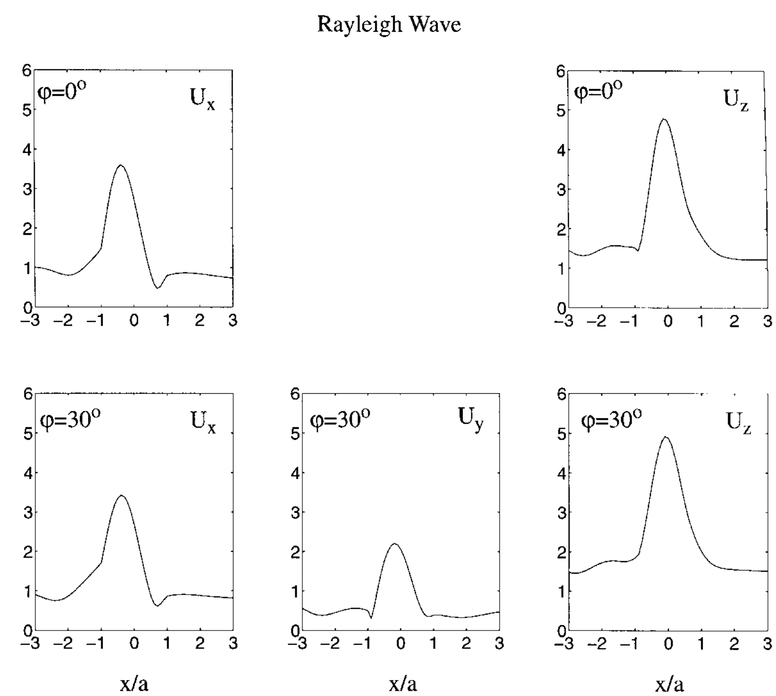

Figure 6. Surface displacement amplitudes of a semi-circular valley of radius a for an incident harmonic Rayleigh wave. $\eta = 0{\cdot}5$, $\varphi = 0$ and 30°

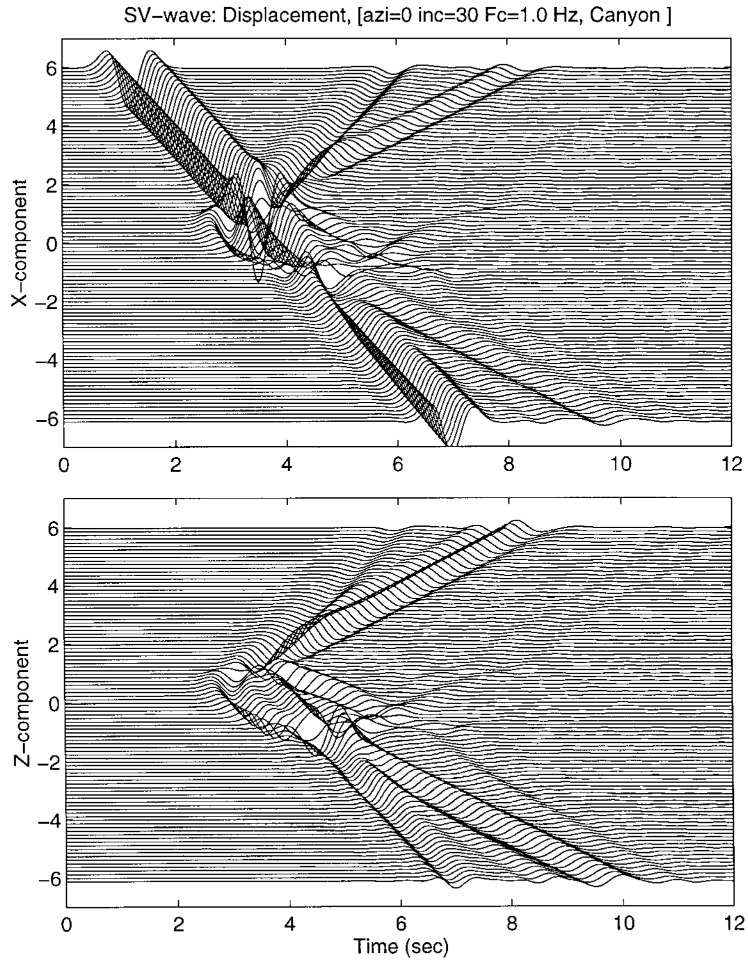

Figure 7. Time–domain displacement response of semi-circular canyon to incident SV ($\varphi = 0°, i = i_c = 30°$) $\left(\nu = \frac{1}{3}\right)$.

SV-waves, $V = \beta/(\sin\, i\, \sin\, \varphi)$; and (iii) for Rayleigh-waves, $V = c_R/\sin,\, \varphi$, where φ and i are the *azimuthal angle* and *angle of incidence*, respectively.

3. VERIFICATION: SCATTERING OF PLANE ELASTIC WAVES BY A SEMICIRCULAR CANYON AND VALLEY

To a certain degree, the method of analysis developed in this paper has already been verified by Luco and de Barros[17] and Pedersen *et al.*[31] who compared results obtained using their own different numerical methods to the results obtained by Pei and Papageorgiou[44,48] (and unpublished results) using the present method. However, for completeness of the presentation we present some additional comparisons with results that have appeared in the published literature. It should be pointed out that the results presented below should not be interpreted as an exhaustive investigation of the physics of the problem (this aspect of the problem will be addressed in a separate paper) but merely as a measure of validity of the method developed in the present paper.

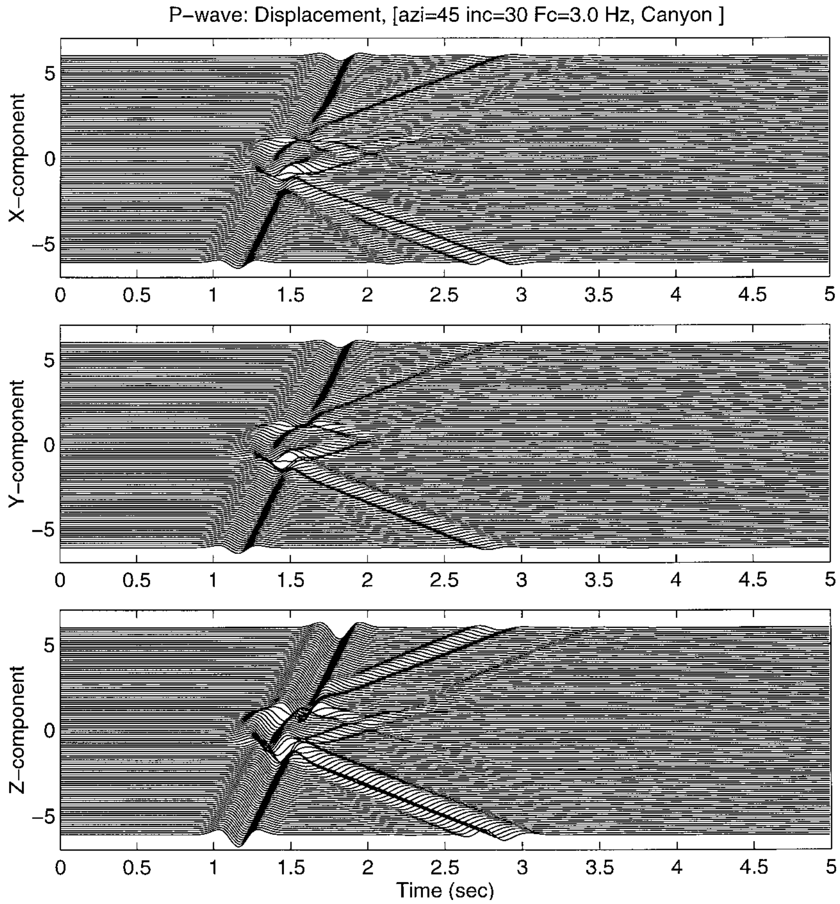

Figure 8. Time–domain displacement response of a semi-circular canyon embedded in a homogeneous half-space to incident P ($\varphi = 45°,\ i = 30°$) wave

3.1. Frequency–domain response of semi-circular Canyon and Valley

The most extensive and thoroughly verified frequency-domain results, related to the 2·5D problem, are those presented by Luco *et al.*[21] for the problem of scattering by topographic irregularity (canyon) and by Luco and de Barros[17] and de Barros and Luco[26] for the problem of scattering by a valley. We validate our method using these results.

Figure 2 displays results for the problem of scattering of body waves by a semi-circular canyon of radius a, which is embedded in a homogeneous half-space characterized by $\alpha = 2\beta$ (i.e. Poisson's ratio $\frac{1}{3}$), and slightly dissipative $\xi_\alpha = \xi_\beta = 0.01$ (where ξ_α and ξ_β represent the small hysteretic damping ratios for P- and S-waves, respectively). The dimensionless frequency $\eta = (\omega a)/(\pi\beta)$ is assumed to be equal to 0·5. The continuous line represents the results obtained by the discrete wavenumber method while the small circles represent the results of Luco *et al.*[21] Of all the cases that we calculated and compared, the one shown in Figure 2 shows the largest discrepancies between our results and those of Luco *et al.* (1990) [22]. Nevertheless, the comparison is still very favourable, with discrepancies that do not exceed 10 per cent and may be attributed to details of discretization of the scatterer. Figure 3 displays results for the same scatterer but for the case when the excitation is an incident Rayleigh wave. The properties of the half-space are the same, except that no damping is considered in this case. However, for the case of Rayleigh

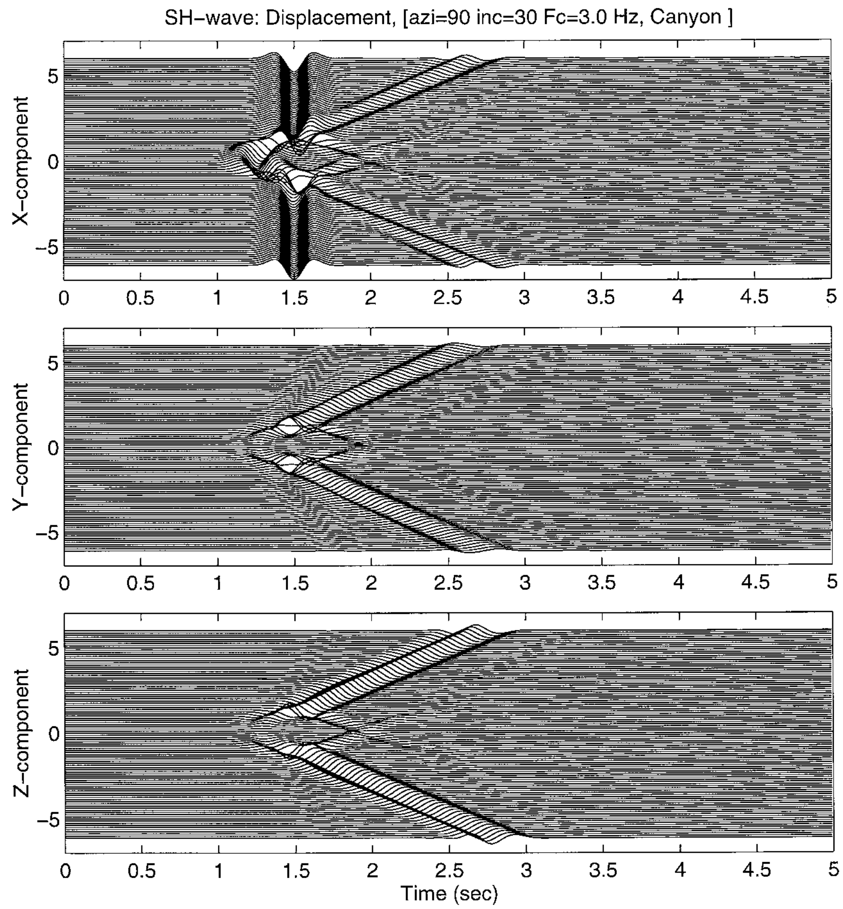

Figure 9. Same as Figure 10, but for incident SH ($\varphi = 90°,\ i = 30°$) wave

wave incident from a nonzero azimuthal direction, no results were available in the published literature for comparison.

Figures 4 and 5 display results for the problem of scattering of body waves by a homogeneous semi-circular valley which is embedded in a homogeneous half-space. The valley (v) and the half-space (h) are characterized by $\alpha_v = 2\beta_v, \alpha_h = 2\beta_h, \alpha_v = \beta_h,\ \rho_v = (2/3)\,\rho_h$ and $\xi_{\alpha h} = \xi_{\beta h} = \xi_{\alpha_v} = \xi_{\beta_v} = 0.005$. Again, as in the previous figures, our results are represented by a continuous line, while those of de Barros and Luco[26] are displayed by small circles. It is evident that the agreement is excellent. (Parenthetically, we should mention that the somewhat larger discrepancies that Luco and de Barros[17] had observed in comparing their results with our unpublished results, should be attributed to differences in the treatment of damping, as the above authors correctly point out in their paper. In the present work special care was taken in treating damping as de Barros and Luco[26] describe in their paper.) Finally, Figure 6 displays results for the valley problem, but for an incident Rayleigh wave. However, no published results were available in the published literature for comparison for the case $\varphi \neq 0$.

3.2. Time–domain response

Figures 7–10 display a sample of time domain responses. In all cases, the time variation of the incident plane wave is described by the Ricker wavelet.[71]

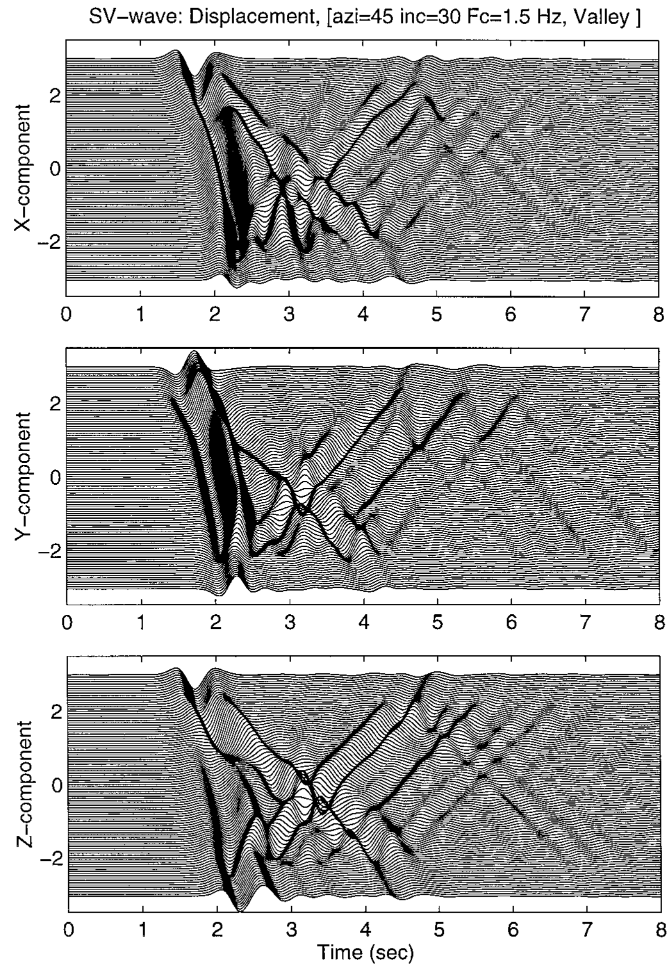

Figure 10. Time–domain displacement response of semi-circular valley to incident SV ($\varphi = 45°,\ i = 30°$)

In Figure 7, we reproduce the results shown in Figure 11 of Kawase,[1] which correspond to the response of a semi-circular canyon to incident SV($\varphi = 0°; i = i_c$) (i_c is the critical incidence angle; for Poisson's ratio $\frac{1}{3}$, $i_c = 30°$). The agreement is excellent.

Figures 8 and 9 display the response of a semi-circular canyon embedded in a homogeneous half-space to incident P ($\varphi = 45°,\ i = 30°$) and SH ($\varphi = 90°,\ i = 30°$) waves. The characteristic frequency f_c of the Ricker wavelet is equal to 3 Hz in both cases. In addition to the diffracted waves that in both cases are observed to propagate on the horizontal surface of the half-space away from the scatterer/canyon, clearly evident are also the *creeping waves*,[1,2] which originate at the edges of the canyon and propagate along the cylindrical surface of the canyon. It is interesting to notice the characteristics of symmetry/antisymmetry of the components of displacement for the case of an SH-wave incident from an azimuthal direction parallel to the long axis of the scatterer (i.e. $\varphi = 90°$; Figure 9). The x-component of displacement is symmetric (with respect to the axis of the canyon), while the other two components are antisymmetric, as anticipated.

Finally, Figure 10 displays the time–domain response of a model of a semi-circular valley to incident SV ($\varphi = 45°, i = 30°$)($f_c = 1{\cdot}5$ Hz). The material properties of the model are the same as those used to obtain the frequency–domain results shown in Figure 5. All three components of motion appear to be equally strong

after the passage of the direct signal, and the seismic energy trapped in the sediments prolongs considerably the duration of the response.

4. CONCLUSION

We have presented and validated a formulation for the "2·5D problem" in elastodynamics. This formulation may be used to study the wavefields in models of sedimentary deposits (e.g. valleys) or topography (e.g. canyons or ridges) with a 2D variation in structure but obliquely incident plane waves. The formulation may also be extended in a straightforward way to accommodate non-planar waves (i.e. sources) in view of the fact that sources may be represented by a summation of plane waves (the Weyl Integral).[65] The advantage of such 2·5D formulations is that they provide the means for calculations of 3D wavefields in scattering problems by requiring a storage comparable to that of the corresponding 2D calculations.

ACKNOWLEDGEMENTS

This work was supported by Contracts No. NCEER 93-2001, 94-2001 and 95-2001, under the auspices of the National Center for Earthquake Engineering Research under NSF Grant No. ECE-86-07591. The research was conducted using the Cornell National Supercomputer Facility (CNSF), a resource of the Center for Theory and Simulations in Science and Engineering (Cornell Theory Center), which receives major funding from the National Science Foundation and IBM Corporation, with additional support from New York State and members of the Corporate Research Institute.

REFERENCES

1. H. Kawase, 'Time-domain response of a semicircular canyon for incident SV, P, and Rayleigh waves calculated by the discrete wavenumber boundary element method', *Bull. Seism. Soc. Am.* **78**, 1415–1437 (1998).
2. J. Kim and A. S. Papageorgiou, 'Discrete wavenumber boundary-element method for 3-D scattering problems', *J. Engng. Mech ASCE* **119**(3), 603–624 (1993).
3. D. M. Boore, 'Finite difference methods for seismic wave propagation in heterogeneous materials', in B. A. Bolt (ed.), *Seismology: Surface Waves and Earth Oscillations* (*Methods in Computational Physics*, Vol. 11) Academic Press, New York, 1972.
4. J. Virieux, 'SH-wave propagation in heterogeneous media: Velocity-stress finite-difference method', *Geophysics* **49**, 1933–1957 (1984).
5. J. E. Vidale and D. V. Helmberger, 'Elastic finite-difference modeling of the 1971 San Francisco, California earthquake', *Bull. Seism. Soc. Am.* **78**, 121–141 (1988).
6. R. W. Graves, 'Simulating wave propagation in 3D elastic media using staggered-grid finite differences', *Bull. Seism. Soc. Am.* **86**, 1091–1106 (1996).
7. J. Lysmer and L. A. Drake, 'A finite element method for seismology', in B. A. Bolt (ed.), *Methods of Computational Physics*, Vol. 11, Academic Press, New York, 1972, pp. 181–216.
8. H. L. Wong and P. C. Jennings, 'Effects of canyon topography on strong ground motion', *Bull. Seism. Soc. Am*. **65**(5), 1239–1257 (1975).
9. M. Bouchon, C. A. Schultz and M. N. ToksÖz, 'Effect of three-dimensional topography on seismic motion', *J. Geophys. Res*. **101**, 5835–5846 (1996).
10. T. K. Mossessian and M. Dravinski, 'A hybrid approach for scattering of elastic waves by three-dimensional irregularities of arbitrary shape', *J. Phys. Earth* **40**(1), 241–261 (1992).
11. J. Regan and D. G. Harkrider, 'Seismic representation theorem coupling: synthetic SH mode sum seismograms for non-homogeneous paths', *Geophys. J.* **98**, 429-446 (1989).
12. T. L. Hong and D. V. Helmberger, 'Glorified optics and wave propagation in(s) nonplanar structures', *Bull. Seism. Soc. Amer.* **68**, 1313–1330 (1978).
13. R. Benites and K. Aki, 'Boundary integral-Gaussian beam method for seismic wave scattering: SH in two-dimensional media', *J. Acoust. Soc. Am.* **86**(1), 375–386 (1989).
14. K. Aki and K. L. Larner, 'Surface motion of a layered medium having an irregular interface due to incident plane SH waves', *J. Geophys. Res.* **75**, 933–954 (1970).
15. K. Koketsu, 'Synthetic seismograms in realistic media: a wave theoretical approach', *Bull. Earthq. Res. Inst (Univ. Tokyo)* **62**, 201–245 (1987).
16. M. Bouchon and O. Coutant, 'Calculation of synthetic seismograms in a laterally-varying medium by the boundary element-discrete wavenumber method', *Bull. Seism. Soc. Am.* **84**, 1869–1881 (1994).
17. J. E. Luco and F. C. P. de Barros, 'Three-dimensional response of a layered cylindrical valley embedded in a layered half-space', *Earthquake Engng. Struct. Dyn.* **24**, 109–125 (1995).
18. J. M. Roesset, in R. J. Hansen (ed.), *Fundamentals of Soil Amplification, Seismic Design for Nuclear Power Plants*, MIT Press, Cambridge, MA., 1970, pp. 183–244.

19. K. B. Olsen, J. C. Pechmann and G. T. Schuster, 'Simulation of 3D elastic wave propagation in the Salt Lake Basin', *Bull. Seism. Soc. Am.* **85**, 1688–1710 (1995).
20. K. B. Olsen and R. J. Archuleta, 'Three-dimensional simulation of earthquakes on the Los Angeles fault system', *Bull. Seism. Soc. Am.* **86**(3), 575–596 (1996).
21. J. E. Luco, H. L. Wong, and F. C. P. De Barros, 'Three-dimensional response of a cylindrical canyon in a layered half-space', *Earthquake Engng. Struct. Dyn.* **19**, 799–817 (1990).
22. F. C. P. de Barros and J. E. Luco, 'Moving Green's functions for a layered viscoelastic half-space', *Report*, Dept. of Appl. Mech. & Engng. Sci., University of California, San Diego, La Jolla, California, 1992, 210pp.
23. F. C. P. de Barros and J. E. Luco, 'Response of a layered viscoelastic half-space to a moving point load', *Wave Motion* **19**, 189–210 (1994).
24. E. Beskos, 'Boundary element methods in dynamic analysis', *Appl. Mech. Rev. ASME* **40**(1), 1–23 (1987).
25. J. E. Luco and F. C. P. de Barros, On the three-dimensional seismic response of a class of cylindrical inclusions embedded in layered media, *Proc. 6th Int. Conf. of Soil Dynamics and Earthquake Engineering*, Bath, U.K., 14–16 June, 1993, pp. 565–580.
26. F. C. P. de Barros, and J. E. Luco, 'Amplification of obliquely incident waves by a cylindrical valley embedded in a layered half-space', *Soil Dyn. Earthquake Engng.* **14**, 163–175 (1995).
27. H. Pedersen, F. J. Sanchez-Sesma and M. Campillo, 'Three-dimensional scattering by two-dimensional topographies', *Bull. Seism. Soc. Am.* **84**, 1169–1183 (1994).
28. F. J. Sanchez-Sesma and M. Campillo, 'Diffraction of P, SV, and Rayleigh waves by topographic features: a boundary integral formulation', *Bull. Seism. Soc. Am.* **81**, 2234–2253 (1991).
29. T. Yokoi and H. Takenaka, 'Treatment of an infinitely extended free surface for indirect formulation of the boundary element method', *J. Phys. Earth* **43**, 79–103 (1995).
30. H. Pedersen, B. LeBrun, D. Hatzfeld, M. Campillo and P.-Y. Bard, 'Ground-motion amplitude across ridges', *Bull. Seism. Soc. Am.* **84**, 1786–1800 (1994).
31. H. A. Pedersen, M. Campillo and F. J. Sanchez-Sesma, 'Azimuth dependent wave amplification in alluvial valleys', *Soil Dyn. Earthquake Engng.* **14**, 289–300 (1995).
32. H. A. Pedersen, V. Maupin and M. Campillo, 'Wave diffraction in multilayered media with the indirect boundary element method: application to 3-D diffraction on long-period surface waves by 2-D lithospheric structures', *Geophys. J. Int.* **125**, 545–558 (1996).
33. H. Takenaka, B. L. N. Kennett and H. Fujiwara, 'Effect of 2-D topography on the 3-D seismic wavefield using a 2·5-D discrete wavenumber-boundary integral equation method', *Geophys. J. Int.* **124**, 741–755 (1996).
34. M. Bouchon, 'A simple, complete numerical solution to the problem of diffraction of SH waves by an irregular surface', *J. Acoust. Soc. Am.* **77**, 1–5 (1985).
35. S. Gaffet and M. Bouchon, 'Effects of two-dimensional topographies using the discrete wavenumber-boundary integral equation method in P-SV cases', *J. Acoust. Soc. Am.* **85**, 2277–2283 (1989).
36. H. Takenaka and B. L. N. Kennett, 'A 2·5-D time-domain elastodynamic equation for plane-wave incidence',*Geophys. J. Int.* **125**, F5–F9 (1996).
37. H. Takenaka and B. L. N. Kennett, 'A 2·5-D time-domain elastodynamic equation for a general anisotropic medium', *Geophys. J. Int.* **127**, F1–F4 (1996b).
38. T. Furumura and H. Takenaka, '2·5-D modelling of elastic waves using the pseudospectral method', *Geophys. J. Int.* **124**, 820–832 (1996).
39. L. Zhang and A. K. Chopra, 'Three-dimensional analysis of spatially varying ground motion around a uniform canyon in a homogeneous half-space', *Earthquake Engng. Struct. Dyn.* **20**, 911–926 (1991a).
40. L. Zhang and A. K. Chopra, 'Impedance functions for three-dimensional foundations supported on an infinitely-long canyon of uniform cross-section in a homogeneous half-space', *Earthquake. Engng. Struct. Dyn.* **20**, 1011–1027 (1991b).
41. K. R. Khair, S. K. Datta and A. H. Shah, 'Amplification of obliquely incident seismic waves by cylindrical alluvial valleys of arbitrary cross-sectional shape. Part I. Incident P and SV waves', *Bull. Seismol. Soc. Am.* **3**, 610–630 (1989).
42. K. R. Khair, S. K. Datta and A. H. Shah, 'Amplification of obliquely incident seismic waves by cylindrical alluvial valleys of arbitrary cross-sectional shape. Part II. Incident SH and Rayleigh waves', *Bull. Seismol. Soc. Am.* **81**, 346–357 (1991).
43. S. W. Liu, S. K. Datta and M. Bouden, 'Scattering of obliquely incident seismic waves by a cylindrical valley in a layered half-space', *Earthquake Engng. Struct. Dyn.* **20**, 859–870 (1991).
44. D. Pei and A. S. Papageorgiou, 'Study of the response of cylindrical alluvial valleys of arbitrary cross-section to obliquely incident seismic waves using the discrete wavenumber boundary element method', *Proc. 6th Int. Conf. of Soil Dynamics and Earthquake Engineering*, Bath, U.K., 14–16 June 1993, pp. 149–161.
45. D. Pei and A. S. Papageorgiou, 'Locally generated surface waves in Santa Clara Valley: Analysis of observations and numerical simulation', *Earthquake Engng. Struct. Dyn.* **25**, 47–63 (1996).
46. A. S. Papageorgiou and D. Pei, '3-D response of cylindrical valleys of arbitrary cross-section to seismic waves incident from any azimuthal direction', *Proc 5th U.S. National Conference on Earthquake Engineering*, 10–14 July 1994, Chicago, ILL, Vol. III, 1994, pp. 45–54.
47. B. Zhang and A. S. Papageorgiou, 'Simulation of the response of the Marina District Basin, San Francisco, California, to the 1989 Loma Prieta earthquake', *Bull. Seism. Soc. Am.* **86**, 1382–1400 (1996).
48. D. Pei and A. S. Papageorgiou, 'Three dimensional response of an infinitely long cylindrical canyon to obliquely incident seismic waves', *Presented at the 88th Annual Meeting of the Seismological Society of America*, 14–16 April 1993, Ixtapa-Zihuatanejo, Mexico; *Seismol. Res. Lett.* **64**(1), 27 (1993).
49. Z. L. Li, J. D. Achenbach, I. Komsky and Y. C. Lee, 'Reflection and transmission of obliquely incident surface waves by an edge of a quarter space: theory and experiment', *ASME J. Appl. Mech.* **59**, 349–355 (1992).
50. R. Courant and D. Hilbert, *Methods of Mathematical Physics*, Vol. 2, Interscience, New York, 1962.

51. R. G. Payton, 'An application of the dynamic Betti-Rayleigh reciprocal theorem to moving-point loads in elastic media', *Quart. Appl. Math.* **21**, 299–313 (1964).
52. A. Eringen and E. S. Suhubi, *Elastodynamics, Vol. II, Linear Theory*, Academic Press, New York, 1975.
53. F. Hartmann, 'Computing the C-matrix in non-smooth boundary points', in C. A. Brebbia (ed.) *New Developments in Boundary Element Method*, CML Publications, Southampton, UK, 1980, pp. 367–379.
54. F. J. Rizzo, D. J. Shippy and M. Rezayat, 'A boundary integral equation method for radiation and scattering of elastic waves in three dimensions', *Int. J. Numer. Meth. Engng.* **21**, 115–129 (1985).
55. J. L. Tassoulas, 'Dynamic soil–structure interaction', in D. Beskos (ed.), *Boundary Element Methods in Structural Analysis*, Chapter 10, ASCE, New York, 1988.
56. Y.-H. Pao and V. Varatharajulu, 'Huygens' principle, radiation conditions and integral formulas for the scattering of elastic waves', *J. Acoust. Soc. Am.* **59**, 1361–1371 (1976).
57. H. Kawase, 'Effects of topography and subsurface irregularities on strong ground motion, *Report 90-02*, Ohsaki Research Institute, Inc.
58. I. R. Gonzalves, D. J. Shippy and F. J. Rizzo, 'Direct boundary integral equations for elastodynamics in 3-D half-spaces', *Computat. Mech.* **6**, 279–292 (1990).
59. B. B. Baker and E. T. Copson, *The Mathematical Theory of Huygens' Principle*, Chelsea Publishing Company, New York, NY, 1939.
60. A. T. de Hoop, 'Representation theorems for the displacement in an elastic solid and their applications to elastodynamic diffraction theory', *D.Sc. Thesis*, Technische Hogeschool, Delft, 1958.
61. A. de Hoop, *Handbook of Radiation and Scattering of Waves*, Academic Press, New York, 1995.
62. P. K. Banerjee and R. Batterfield, *Boundary Element Methods in Engineering Science*, McGraw-Hill, London, 1981.
63. J. Dominguez, *Boundary Elements in Dynamics*, Elsevier, London, 1993.
64. H. Lamb, 'On the propagation of tremors over the surface of an elastic solid', *Phil. Trans. Roy. Soc. London* **A203**, 1–42 (1904).
65. M. Bouchon, 'Discrete wave number representation of elastic wave fields in three-space dimensions', *J. Geophys. Res.* **84**, 3609–3614 (1979).
66. R. Burridge and L. Knopoff, 'Body force equivalents for seismic dislocations', *Bull. Seism. Soc. Am.* **54**, 1874–1888 (1964).
67. K. Aki and P. G. Richards, *Quantitative Seismology, Theory and Methods*, W. H. Freeman, New York, 1980.
68. N. W. McLachlan, *Bessel Functions for Engineers*, 2nd Edn, Oxford University Press, London, 1961.
69. D. Pei, 'Study of the 3-D response of 2-D scatterers: earthquake engineering applications', *Ph.D. Thesis*, Rensselaer Polytechnic Institute, Troy, New York, 1997.
70. H. Kawase and K. Aki, 'A study on the response of a soft basin for incident S, P, and Rayleigh waves with special reference to the long duration observed in Mexico City', *Bull. Seism. Soc. Am.* **79**, 1361–1382 (1989).
71. N. Ricker, 'The computation of output disturbances from amplifiers for true wavelet inputs', *Geophysics* **10**, 207–220 (1945).
72. F. J. Sanchez-Sesma and M. Campillo, 'Topographic effects for incident P, SV and Rayleigh waves', *Tectonophysics* **218**, 113–125 (1993).
73. H. L. Wong, 'Effect of surface topography on the diffraction of P, SV and Rayleigh waves', *Bull. Seism. Soc. Am.* **72**, 1167–1183 (1982).

